Localizing the osseous boundaries of micro-osteoperforations

Lauren N. van Gemert,[a] Phillip M. Campbell,[b] Lynne A. Opperman,[c] and Peter H. Buschang[b]
Spokane, Wash, and Dallas, Texas

Introduction: The aim of this work was to determine how far the effects of micro-osteoperforations (MOPs) extend within bone by quantifying the damage caused and the short-term bony adaptations that occur in and around the injury site. **Methods:** With the use of a split-mouth design, 34 MOPs (Propel) were randomly placed in the mandibular furcal bone of 13 beagle dogs either 2 or 4 weeks before killing them. The control side received no treatment. Vickers hardness microindentation, microscopic computed tomography, and histologic analyses were performed to evaluate the bone surrounding the MOPs. **Results:** Microfractures produced during insertion extended ~0.6 mm from the MOP sites. Cortical and trabecular bone were significantly less dense on the experimental than on the control side up to 4.2 mm from the edge of the MOP, but side differences were small (<5%) beyond 1.5 mm from the MOP. Experimental cortical bone was significantly softer than the control bone up to 0.8 mm from the MOP after 2 weeks of healing, and up to 0.5 mm from the MOP after 4 weeks of healing. Hematoxylin and eosin stained sections of cortical and trabecular bone showed small areas of woven bone within the MOP sites after 2 weeks, and acellular areas of bone extending ~0.5 mm from the MOP. After 4 weeks of healing, there were greater amounts of woven bone, as well as early signs of lamellar bone, in and around the MOP sites. Markedly increased TRAP activity extending up to 2.5 mm from the MOP was evident after 2 weeks, but not after 4 weeks. Vital fluorescence staining showed diffuse bone deposition on the experimental side up to 1.5 mm from the MOP margin. **Conclusions:** When MOPs are performed in beagle dogs, demineralization is transient and healing of the injured area, as well as remineralization of bone affected by MOP placement, begins during the first 2 weeks. Although the transient effects extend farther, the principal effects extend only ~1.5 mm from the MOP site. (Am J Orthod Dentofacial Orthop 2019;155:779-90)

Fixed orthodontic treatment takes ~21-27 months for nonextraction cases and ~25-35 months for extraction cases.[1] Variation in treatment time among patients depends on various factors, including the amount of tooth movement required, the mechanics used, and the degree of patient cooperation.[2,3] Efforts must be made to shorten orthodontic treatments because longer durations increase the risks of white spot lesions, dental caries, root resorption, and gingival inflammation.[1,4-6]

[a]Private practice, Spokane, Wash.
[b]Department of Orthodontics, Texas A&M University College of Dentistry, Dallas, Texas.
[c]Department of Biomedical Sciences, Texas A&M University College of Dentistry, Dallas, Texas.
All authors have completed and submitted the ICMJE Form for Disclosure of Potential Conflicts of Interest, and none were reported.
Address correspondence to: Peter H. Buschang, Professor and Director of Orthodontic Research, Orthodontic Department, Texas A&M University College of Dentistry, Dallas, TX; e-mail, phbuschang@tamhsc.edu.
Submitted, May 2017; revised and accepted, July 2018.
0889-5406/$36.00

https://doi.org/10.1016/j.ajodo.2018.07.022

The average rate of conventional orthodontic tooth movement is ~1 mm per month.[7-9] To minimize the consequences of extended treatment times, as well as to satisfy many patients' desire for faster treatment, new techniques focusing on increasing tooth movements have become popular over the past decade. Traumatizing bone increases rates of tooth movement by initiating the regional acceleratory phenomenon (RAP) and accelerating rates of bone turnover.[10-12] Corticotomy-based surgeries are the most commonly used method to induce the RAP effect,[11-13] but because of their invasiveness there has been recent interest in less invasive techniques.

Micro-osteoperforations (MOPs), which penetrate through the gingiva and into the cortical bone adjacent to teeth, are currently being marketed to accelerate tooth movements. The most common technique uses the Propel device (Propel Orthodontics, Milpitas, Calif), a 1.4-mm surgical stainless steel miniscrew implant attached to a driver, to create MOPs. Clinically, the technique has been shown to double the rate of tooth movements,[14] but that study's duration was limited and part of the treatment effect appears to have been due to

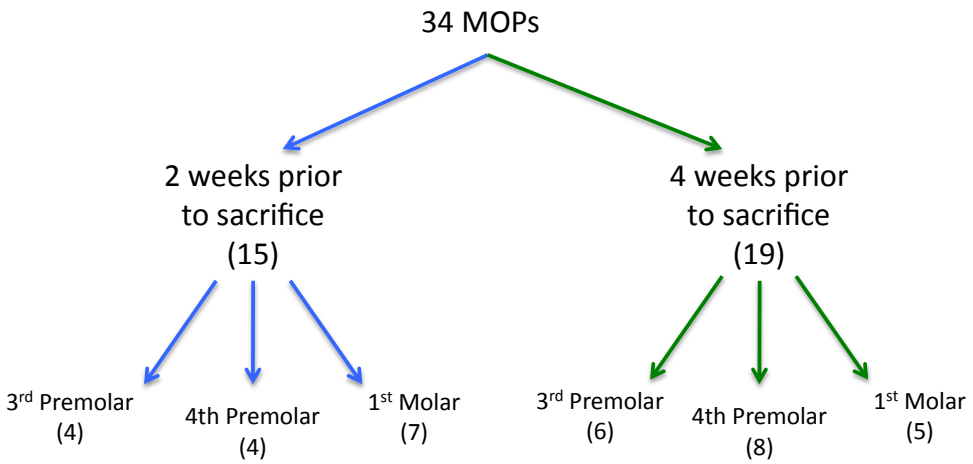

Fig 1. MOP designations. Summary of MOPs placed for each duration and location. A total of 34 MOPs were placed over the course of the experiment; 15 MOPs were placed 2 weeks before the dogs were killed and 19 MOPs were placed 4 weeks before.

tipping. The experimental literature evaluating the effectiveness of the MOPs remains controversial.[15-18]

The short-term effects of MOPs on cortical and trabecular bone have not been previously investigated. Most importantly, it remains unknown how far the effects of MOPs extend within bone. The purpose of the present study was to evaluate the amount of damage induced by MOPs and quantify the extent of the subsequent remodeling that occurs in and around the injury site. The goal is to understand why MOPs may not be effective in accelerating tooth movements.[19,20]

MATERIAL AND METHODS

This experiment used 13 skeletally mature male beagle dogs, each ~2 years of age and weighing 21-25 pounds. Dogs were used because their teeth, periodontal ligaments, and alveolar bone qualities are similar to those of humans.[21-23] The Institutional Animal Care and Use Committee approved the experimental protocol.

After 10 days of quarantine, the animals were sedated, received dental prophylaxis, and had periapical radiographs taken of the right and left sides of the mandible, including the teeth, to determine MOP sites. There had to be at least 2 mm of bone between the roots of the teeth.

After sedation with a ketamine and xylazine mixture, local anesthesia was administered and the MOPs were performed in the furcal bone of the experimental mandibular third premolars, fourth premolars, and first molars.

The MOPs were performed with the use of the Propel device from buccal to lingual, at a depth of 7 mm, or to the lingual cortical plate. After placement, periapical and occlusal radiographs were taken. The Propel miniscrew was then removed and the trauma site was cleaned with the use of 2% chlorhexidine gluconate gel.

Each dog received 3 MOPs, except in those cases where the mental nerve was located in the furcation of the third premolar. Each animal's mandibular third premolars, fourth premolars, and first molars were randomly allocated to either the experimental (MOP) or control (no MOP) side (Fig 1). The teeth were also randomly allocated to have MOPs placed either 2 or 4 weeks before the dogs were killed. A total of 34 MOPs were performed, 15 2 weeks before and 19 4 weeks before the dogs were killed. In one animal, 6 MOPs were performed immediately before it was killed in the furcations of the mandibular third premolar, fourth premolar, and first molar.

Calcein green was administered intravenously on days 0 and 24, and alizarin red was administered intravenously on day 14. All of the dyes were prepared immediately before their use. At the end of the 4-week experimental timeline, the animals were killed. The mandibles were harvested, initially stored in 4% paraformaldehyde (PFA) and then after 2 weeks placed in 0.5% PFA for long-term storage.

The mandibles were sectioned to produce blocks ~15 mm wide and 25 mm long, each including the third premolar, fourth premolar, and first molar, as well as the furcal bone from the alveolar crest to the mandibular border. Two bone blocks were placed in 27-mm-wide microscopic computed tomography (μCT) tubes, immersed in 0.5% PFA, tightly sealed with Parafilm, loaded into a ScanCo Micro-CT 35 scanner and scanned at 30 μm resolution, 55 kVp voltage, 145 μA current, and 600 ms integration time.

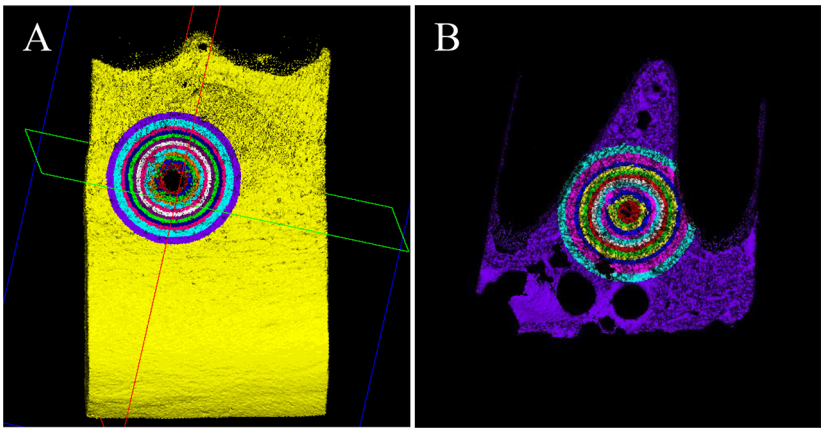

Fig 2. 3D μCT reconstructions for evaluating bone density: buccal view. 3D reconstructions of the block sections were used to determine the density of **A,** cortical bone and **B,** trabecular bone at increasing distances (0.3-mm intervals) from the MOP. The outermost ring of evaluation extended 4.2 mm.

Three-dimensional (3D) reconstructions of the block specimens were completed by 1 investigator with the use of Analyze 12.0 software. The cortical bone volume of interest was defined with a series of 3D spheres that began at the edge of the MOP, and radiated outward for 4.2 mm at intervals of 0.3 mm (Fig 2, *A*). For each sphere, the intensity of the buccal cortical bone was measured and converted to density (density = 0.9361 × intensity + 1041) based on the software manufacturer's recommendations. For trabecular density, a thin section of the bone, with a buccolingual thickness approximately equivalent to the size of the MOP, was isolated (Fig 2, *B*), and a series of 3D spheres (0.3 mm apart) were created, also extending 4.2 mm from the MOP. Any teeth included within the spheres were segmented out so that only bone density was calculated.

The MOPs performed immediately before the dog was killed were stained with a $BaSO_4$ precipitate, in which the barium and sulfate ions diffused into the void spaces present in the bone.[17,24] Specimens were bathed in a solution of equal parts buffered saline, acetone, and 0.5 mol/L $BaCl_2$ (certified ACS crystal; Fisher Scientific, Fair Lawn, NJ) in distilled water for 3 days under vacuum pressure (~50 mm Hg). They were then rinsed and placed in a new solution composed of equal parts buffered saline, acetone, and 0.5 mol/L $NaSO_4$ (anhydrous powder; Fisher Scientific) in deionized water for 3 days under vacuum pressure (~50 mm Hg). The specimens were then rinsed and imaged with the use of the μCT scanner at 10.0 μm resolution, 70 kVp voltage, 114 μA current, and 600 ms integration time.

With the use of Analyze 12.0, the lengths of microfractures were measured linearly from the edge of the MOP to the farthest extent of the precipitate; the measurements were scaled based on the known diameter of the MOP (1.4 mm). Using the sagittal plane, 4 measurements were taken at each MOP and averaged to obtain the approximate mean crack length.

The hardness of cortical bone was measured with the use of a FM-1e Digital Microhardness Tester by 1 blinded investigator. Each sample was sectioned from buccal to lingual through the site of injury with a Buehler Isomet low-speed saw (Lake Bluff, Ill) to expose the affected tissue. The control samples were sectioned in the same manner, at the same location on the other side of the jaw.

The samples were embedded in orthodontic resin (Dentsply), polished with a Economet 3 Variable-Speed Grinder-Polisher using a series of sandpaper discs (200, 400, 600, 800, and 1200 grit), and microhardness was tested from the MOP to a distance of 5 mm, at intervals of 150 μm. A Vickers diamond probe was used at 50 gf with a dwell time of 15 seconds.[25,26] Calibration was performed with the use of steel samples of known hardness provided by the manufacturer. The size of each indentation was measured and the Vickers hardness (HV) of each sample was calculated based on the formula $HV = 1.8544 \times F/d^2$, where F represents the force in kg and d represents the size of the diagonal of the indentation in mm.

Twelve experimental (six 2-week samples and six 4-week samples) and 6 control samples were submitted to fluorescent microscopy with the use of sagittal oriented slices. An additional 12 experimental (six 2-week

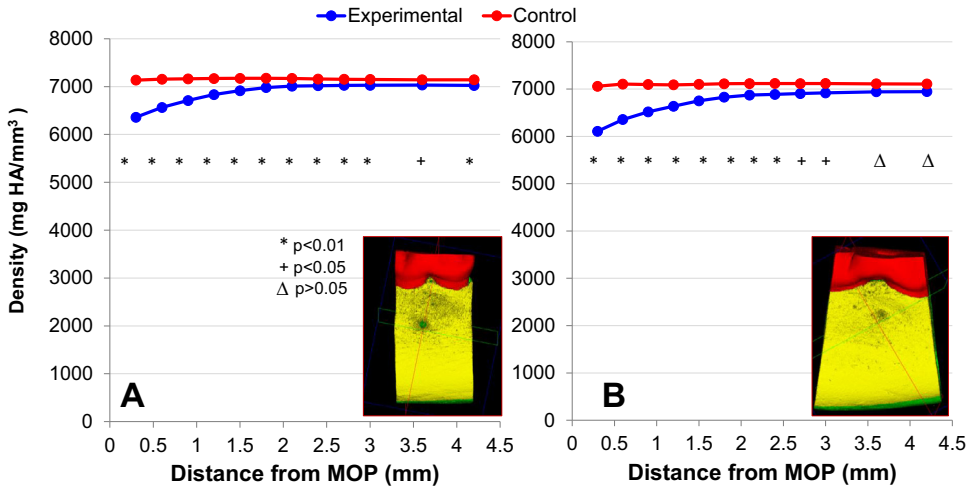

Fig 3. Cortical bone density after **A,** 2 weeks and **B,** 4 weeks of healing. Density (mg HA/mm^3) change in buccal cortical bone at increasing millimeter distances from MOP edge.

samples and six 4-week samples) and 6 control samples were evaluated with the use of traditional hematoxylin and eosin (H&E) stains and tartrate-resistant acid phosphatase (TRAP) stain on slices obtained in a coronal orientation.

To evaluate the fluorescent dyes, the specimens were fixed in 4% PFA, dehydrated with an ascending series of alcohols, embedded in methyl methacrylate, and allowed to polymerize. They were sectioned from buccal to lingual with the use of the Isomet low-speed saw at a thickness of ~150 μm, hand-ground to a thickness of ~100 μm, and mounted on coated glass slides and polished. The images were digitized with the use of a Nikon Eclipse 80i microscope (www.nikonmetrology.com) at a magnification of ×5.

The samples used for H&E and TRAP staining were fixed in 4% PFA, decalcified in EDTA, dehydrated through a graded series of alcohols, cleared with xylene, and then infiltrated with, and embedded in, paraffin. The blocks were sectioned with the use of a microtome to a thickness of 7.5 μm, mounted on coated glass slides, stained with either H&E or TRAP, visualized under a Zeiss Axioplan microscope (Carl Zeiss Microscopy, Thornwood, NY), and photographed with the use of SPOT 5.0 software (www.spotimaging.com).

Statistical analysis and determination of significance

Multilevel statistical models[27] were used to statistically evaluate between-side differences in bone density and microhardness. Two-level models were used to partition variation between animals at the higher level and between sides at the lower level. The experimental and control specimens were compared with the use of a significance level of $P < 0.05$.

RESULTS

After surgery, the MOP sites healed normally with little to no swelling and no infections in any of the animals. All soft tissue trauma caused by MOP placement was healed within 2 weeks of the procedure.

The 3D reconstructions showed distinct holes where the MOPs were placed after 2 weeks, as well as a significant amount of bone in the hole produced by the MOP after 4 weeks of healing (Fig 3). After 2 weeks, buccal cortical bone near the MOP sites was significantly less dense than control bone up to 4.2 mm from the MOP site. Differences in cortical bone density decreased with increasing distances from the MOP (Fig 3). Beyond 1.2 mm, differences between experimental and control bone density were less than 5%. After 4 weeks of healing, cortical bone density was also significantly less on the experimental than control sides up to 3.0 mm from the MOP edge. Beyond 1.5 mm from the MOP edge, the differences between the experimental and control densities were again less than 5%.

Trabecular bone density was significantly less on the experimental side up to 4.2 mm from the MOP after 2 weeks, and for up to 2.1 mm after 4 weeks of healing (Fig 4). Differences were less than 5% beyond 0.9 mm and 1.2 mm from the MOP edge after 2 and 4 weeks, respectively.

The microfractures created by the MOP were clearly evident on the μCT sections (Fig 5). The longest cracks extended ~0.8 mm from the MOP. The mean crack length was 0.6 mm.

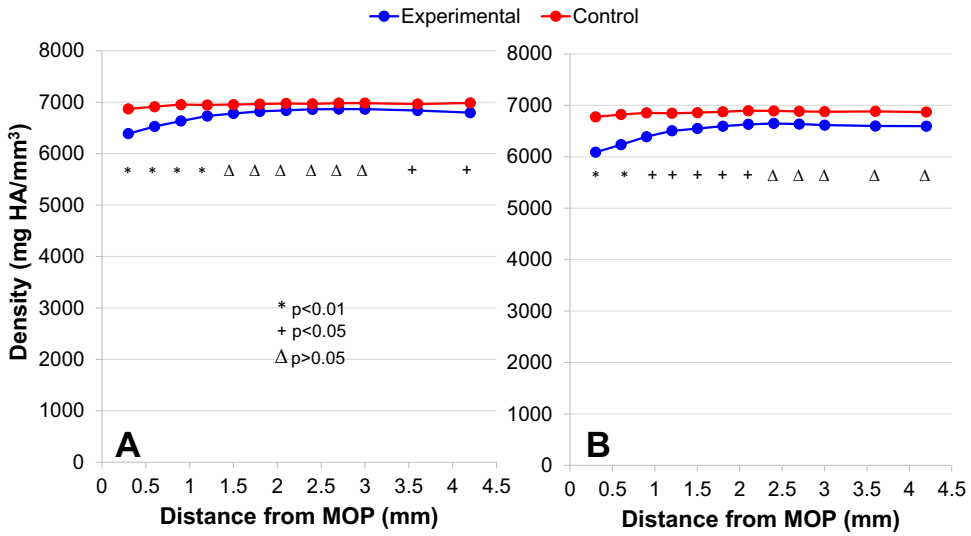

Fig 4. Trabecular bone density after **A,** 2 weeks and **B,** 4 weeks of healing. Density (mg HA/mm^3) change in trabecular bone at increasing millimeter distances from MOP edge.

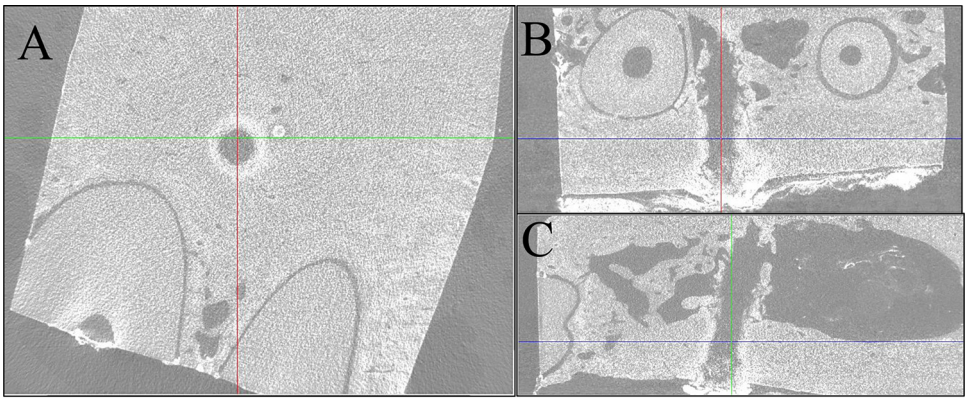

Fig 5. μCT sections used to visualize microfracture pattern. **A,** Sagittal, **B,** axial, and **C,** coronal views of 3Dl μCT volume used for microfracture pattern analysis. The microfractures produced by placement of the Propel miniscrew are seen immediately surrounding the MOP site in all 3 views. Microfractures were stained with the use of a precipitate reaction before μCT analysis, which created a grayscale threshold difference to allow for visualization.

Two-week experimental cortical bone was significantly softer than control cortical bone up to 0.75 mm from the edges of the MOPs (Fig 6). The 4-week specimens showed statistically significant differences in hardness up to 0.45 mm from the edges of the MOPs.

The H&E sections of cortical bone (Fig 7), showed large numbers of osteoblasts and small areas of woven bone within the MOP sites after 2 weeks of healing. There also were acellular areas of bone, devoid of osteocytes and with large numbers of empty osteocyte lacunae, extending ~0.5 mm from the MOP sites. After 4 weeks of healing, there were greater amounts of woven bone within the MOP site. Areas of remodeling at 4 weeks were significantly smaller and fewer in number. In addition, there were new osteocytes and early signs of lamellar bone within and immediately adjacent to the MOP site. However, some empty osteocyte lacunae remained and not all of the acellular bone adjacent to the MOP site had been remodeled. Similar areas of acellular bone were not found in the control bone.

Within the trabecular bone (Fig 8), increases in the amount of bone and decreases in the trabecular size immediately surrounding the MOP site were evident after 2 and 4 weeks. Farther from the MOP site, the trabecular patterns mirrored those of the control bone. After 2 weeks of healing, there were large numbers of osteoblasts lining

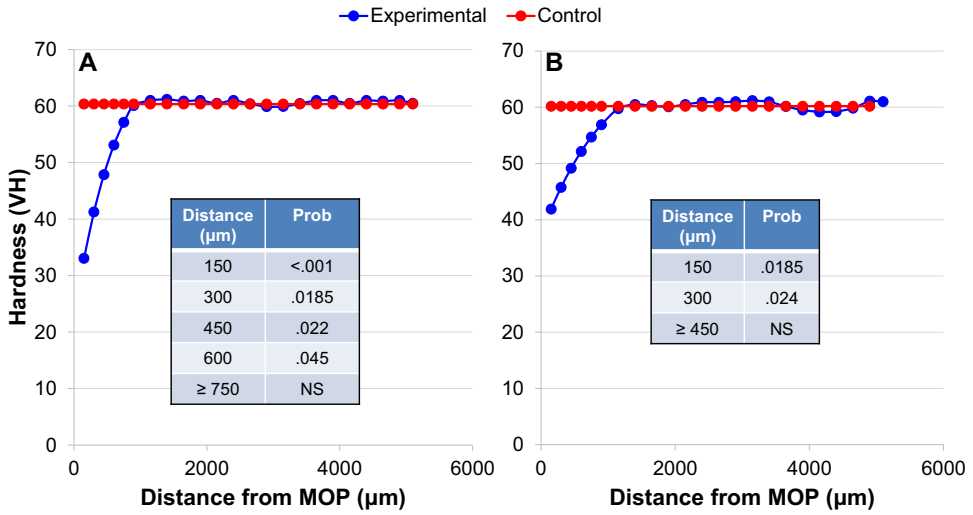

Fig 6. Cortical bone hardness after **A,** 2 weeks and **B,** 4 weeks of healing. Vickers hardness (VH) of buccal cortical bone at increasing micrometer distances from MOP edge.

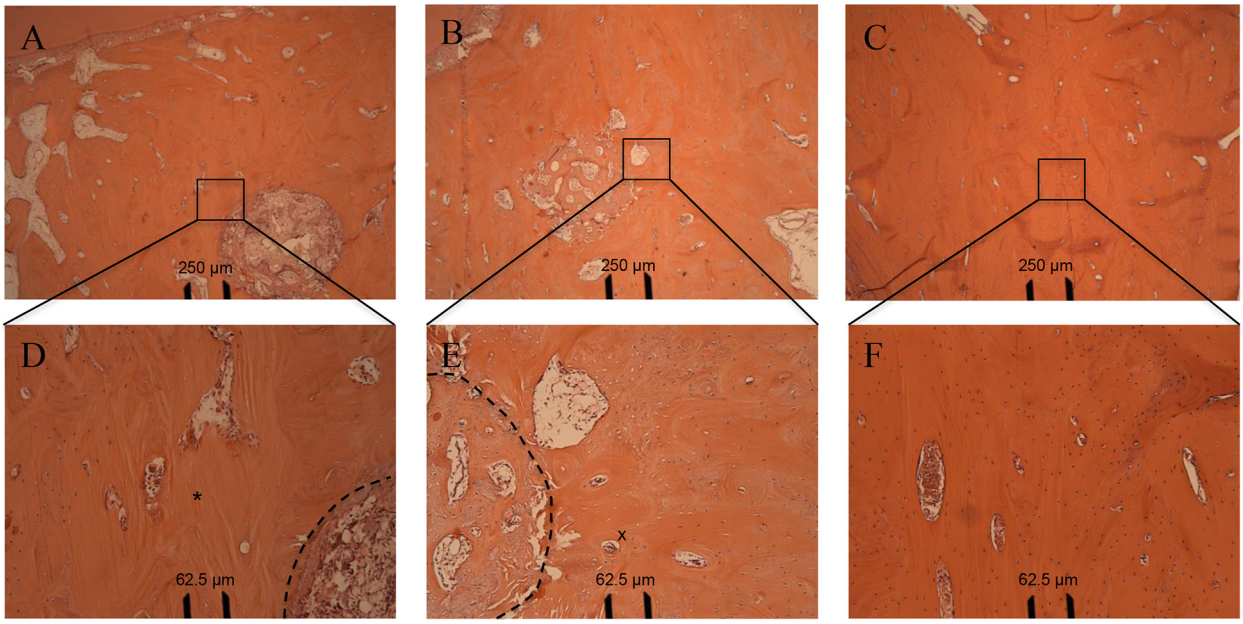

Fig 7. H&E staining: cortical bone. ×2.5 magnification of MOP site and surrounding cortical bone after **A,** 2 weeks and **B,** 4 weeks of healing, compared with **C,** control bone. **D,** After 2 weeks of healing (×10 magnification), a large numbers of osteoblasts and small areas of woven bone are present within the MOP hole (*dashed outline*). In addition, there is an area of dead bone (*) immediately adjacent to the MOP that is devoid of osteocytes. **E,** After 4 weeks of healing (×10 magnification), there is a significant amount of woven bone within the MOP site (*dashed outline*), as well as new osteocytes, woven bone and some early signs of lamellar bone in the area immediately adjacent to the MOP (*x*). **F,** ×10 magnification of control bone.

areas of demineralization, as well as small areas of woven bone within the MOP site. Similarly to the cortical bone, there was an area devoid of osteocytes (empty lacunae visible at ×10 magnification) immediately adjacent and extending slightly less than 0.5 mm from the MOP site. After 4 weeks of healing, there were increased amounts of new woven bone within and immediately surrounding the MOP site. In addition, both the MOP site and the

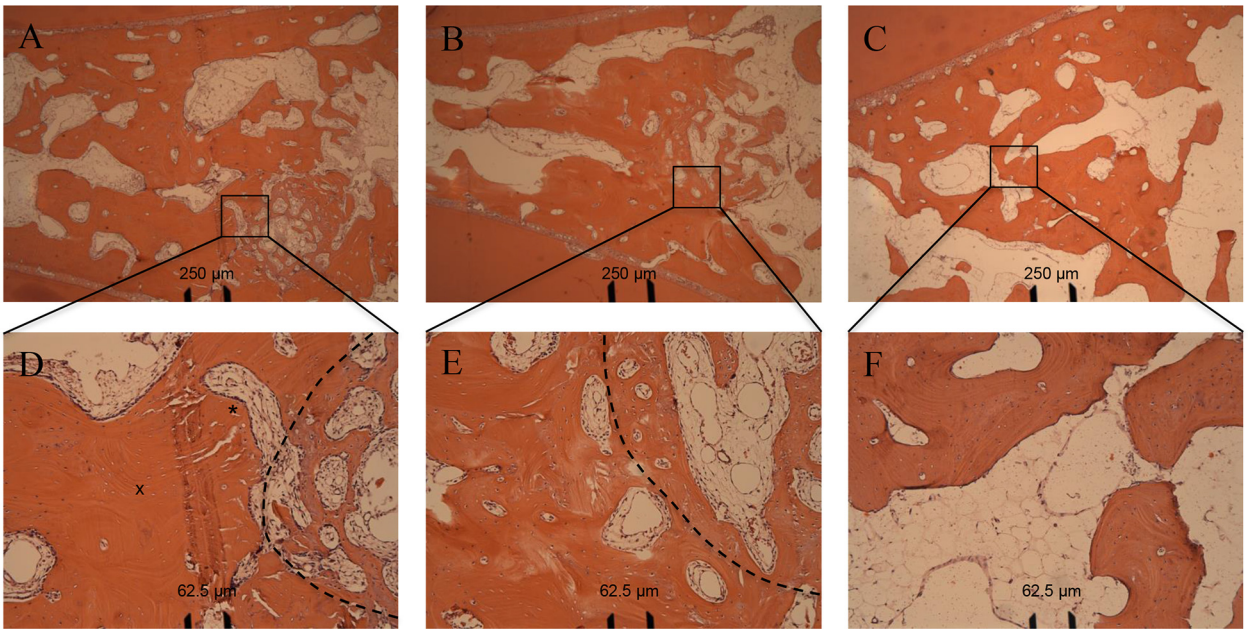

Fig 8. H&E staining: trabecular bone. ×2.5 magnification of MOP site and surrounding trabecular bone after **A,** 2 weeks and **B,** 4 weeks of healing, compared with **C,** control bone. **D,** After 2 weeks of healing (×10 magnification), less trabeculation is present around the MOP (outlined), large numbers of osteoblasts (*), and areas of woven bone present within the MOP (*dashed outline*). In addition, there is an area of dead bone devoid of osteocytes immediate adjacent to the MOP (*x*). **E,** After 4 weeks of healing, there continues to be significantly less trabeculation around the MOP site (*dashed outline*) as well as an increase in the amount of new woven bone in the MOP and immediately surrounding. **F,** ×10 magnification of control bone.

bone adjacent to it showed multiple new osteocytes and small areas of newly formed lamellar bone.

Histologic sections stained with TRAP showed greater osteoclastic activity after 2 weeks in experimental than in control cortical bone (Fig 9). The 2-week experimental bone showed extensive TRAP activity within and beyond the MOP sites, extending ~2.6 mm. The TRAP activity around the MOP sites had declined to control levels after 4 weeks; some TRAP activity was evident within the MOP site. TRAP staining of the trabecular bone also showed increased TRAP activity after 2 weeks within the MOP site and extending ~2.5 mm from the edges of the MOPs. After 4 weeks of healing, TRAP activity was still elevated in the MOP site, and normal TRAP activity was evident in bone surrounding the MOP, similarly to the control site.

Two weeks after MOP placement, cortical bone (Fig 10) showed increased amounts of diffuse calcein labeling around the MOP, extending ~0.8-1.0 mm. After 4 weeks, there had been more new mineral deposited within the MOP site, extending ~1.0-1.5 mm from the edge of the MOP. Beyond this, mineralization of the experimental and control samples was similar. In addition to greater amounts of fluorescence (new mineral deposition) in the MOP holes, there was less space between areas of mineralization in both the 2- and 4-week experimental samples.

Although the patterns of mineralization were similar, there were greater areas of mineralization in trabecular than in cortical bone. Mineralization was evident within and immediately adjacent to the MOP sites after 2 weeks. The greatest differences in mineralization within the trabecular bone was evident after 4 weeks of healing. There was also significantly greater mineralization within the MOP sites after 4 weeks, again extending ~1.0-1.5 mm from the edge of the MOP. Beyond 1.5 mm, the fluorescence labels showed mineralization levels similar to the control specimens.

DISCUSSION

The effects of MOPs on bone appears to be transient. TRAP activity within the MOP sites, and up to 2.5 mm away, was significantly increased after 2 weeks of healing in both the cortical and trabecular bone, but declined to control levels after 4 weeks. However, the

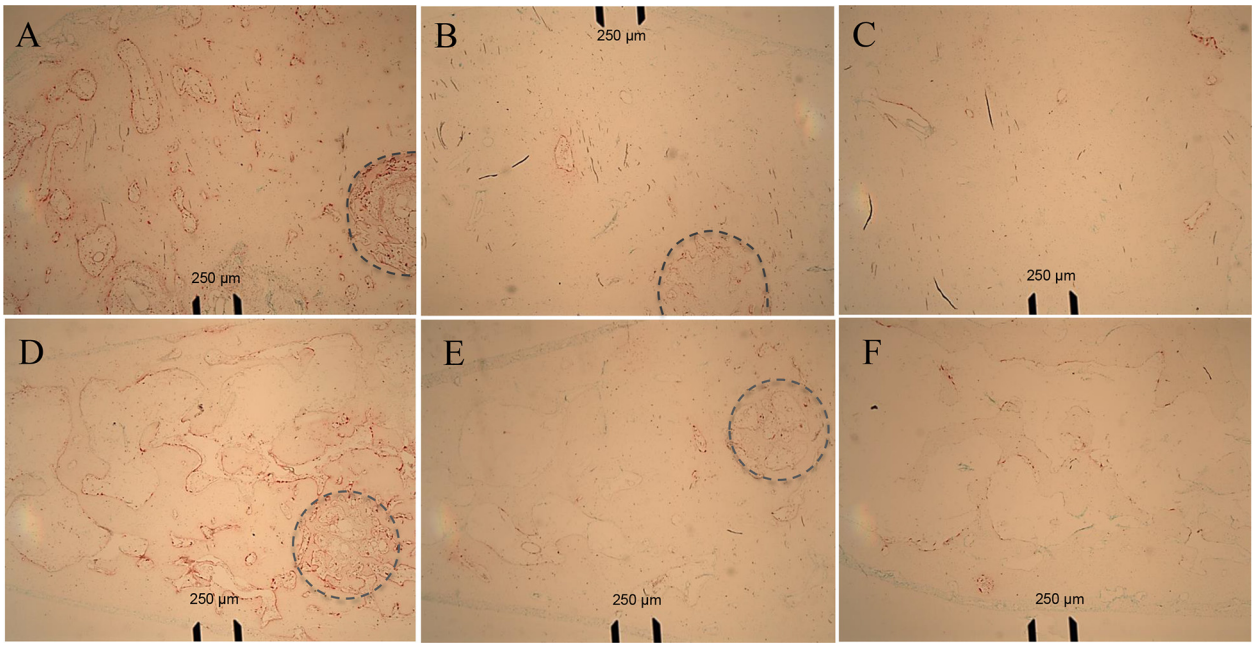

Fig 9. TRAP staining: ×2.5 magnification of osteoclastic activity within **A,** 2-week buccal cortical bone, **B,** 4-week buccal cortical bone, **C,** control buccal cortical bone, **D,** 2-week trabecular bone, **E,** 4-week trabecular bone, and **F,** control trabecular bone. Note the increases in osteoclastic activity within the MOP site (*dashed outline*) as well as at the extensive area of activity after 2 weeks of healing. After 4 weeks of healing, the only area of increased activity was within the MOP site.

experimental cortical and trabecular bone was slightly less dense after 4 than after 2 weeks. Together, these results suggest that the duration of the demineralization event produced by MOPs is limited, with most of the effects occurring during the first few weeks. Previous experimental results support the fact that demineralization continues for ~3 weeks following piezocision.[28] Studies evaluating the effects of corticotomies in beagle dogs have shown differences between experimental and control rates of tooth movement for ~3 weeks, after which differences in tooth movement, and presumably demineralization, decreased.[13,29,30] This is clinically important because it implies that the greatest effects on tooth movement should be expected within the first 3 weeks following MOP placement. An experimental split-mouth study recently showed that there might be a slight effect of MOPs on tooth movements during the first few weeks.[20]

Healing in the MOP begins soon after the trauma. The histologic sections showed increased numbers of osteoblasts and woven bone within the MOP sites after 2 weeks. After 4 weeks of healing, there were large areas of woven bone and early lamellar bone. The fluorescence data showed bone mineralization within the MOP sites after 2 weeks, and more dramatic amounts of mineralization after 4 weeks. Kim et al[31] also reported early healing, with osteoblasts present 7 days after corticision, and increased numbers of osteoblasts and osteocytes in actively forming bone matrix by day 14. In contrast, osteoclastic activity in the MOP was much greater after 2 than after 4 weeks. Although remineralization and demineralization within the MOP site occur simultaneously, demineralization predominates initially and was of more limited duration. MOP sites have been shown to be nearly, but not completely, healed after 7 weeks.[20]

The areas around the MOP sites showed similar patterns of healing. Fluorescence showed moderate diffuse mineral deposition immediately adjacent to the MOP sites after 2 weeks, and more pronounced mineralization a short distance away after 4 weeks, especially in trabecular bone. Demineralization of bone around the MOP sites, which was clearly evident after 2 weeks, had returned to control levels after 4 weeks. Cortical microhardness near the MOP sites was greater after 4 than after 2 weeks, indicating healing of the microfractures. De novo bone formation around endosseous implants is initiated 1 week after placement, with marked new bone formation along most implant surfaces after 2 weeks and significant amounts of woven and lamellar bone after 4 weeks.[32]

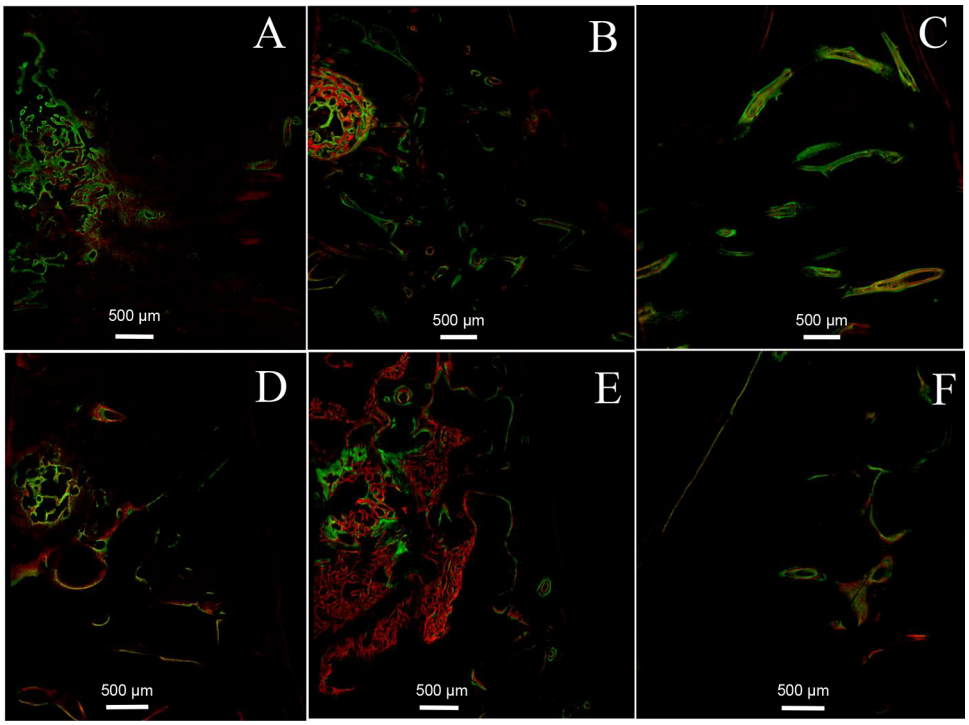

Fig 10. Fluorescence microscopy: cortical bone. Vital staining (×2.5 magnification) with calcein (*green*) and alizarin (*red*) bone labels. **A,** Cortical bone after 2 weeks, **B,** cortical bone after 4 weeks, **C,** control cortical bone, **D,** trabecular after 2 weeks, **E,** trabecular bone after 4 weeks, and **F,** control trabecular bone.

Normal trabecular healing occurs after MOP placement. The H&E sections demonstrated greater amounts of woven bone, as well as decreases in the size of the trabeculae immediately surrounding the MOP site after both 2 and 4 weeks. Fractures within trabecular bone are typically repaired through intramembranous ossification, with bone being laid down directly onto areas of existing bone.[33] In the present study, the trabeculae were smaller in the experimental than the control bone. Greater numbers of trabeculae, thinner trabeculae, and less trabecular separation have been associated with newly formed bone.[34-36] The presence of woven bone with smaller trabecular size in and adjacent to the MOP sites in the present study indicates that the bone was newly laid down as part of the normal repair process.

Unexpectedly, placement of MOPs in the cortical and trabecular bone produced extensive acellular areas extending ~0.40 mm from the edge of the MOP. This distance corresponds well with the extent of the microfractures observed in the present study. The acellular areas were devoid of osteocytes 2 weeks after MOP placement, with numerous empty osteocyte lacunae. After 4 weeks of healing, many empty osteocyte lacunae remained in both the cortical and trabecular bone, but there were early signs of lamellar bone with new osteocytes dispersed within the acellular areas. This finding can be explained by the extensive filopodial network within the canaliculi of the mineralized bone that allows osteocytes to communicate.[37] They deform in response to changes in the fluid flow within the canaliculi induced by mechanical strains placed on the bone.[38] Studies evaluating bone strain after the placement of self-tapping miniscrew implants (similar to the screws used to create the MOPs) have shown strains above the physiologic limits of the bone extending 0.10-0.50 mm into the bone.[39,40] There are also significant decreases in fluid shear stress associated with microcracks, leading to further osteocyte apoptosis.[37,41,42] The acellular bone identified immediately adjacent to the MOP is similar to the hyalinized zones adjacent to the periodontal ligament seen during orthodontic tooth movement.[43] Hyalinization limits tooth movement for 2-4 weeks because the dead osteocytes in these areas are not able to recruit osteoclasts to participate in bone remodeling.[44] It is possible that areas of acellular bone around the MOP sites may also inhibit tooth movements, possibly negating the demineralization induced adjacent to the MOP placement site.

The extent of the microdamage and the greatest effects on bone produced by the Propel device appear to extend no more than 1.5 mm from the MOP site. Microfractures in the present study extended no more than 0.8 mm from the MOP. Self-drilling miniscrew implants, with diameters similar to the PROPEL device used in the present study, produce microcracks in the cortical bone extending 0.75 mm at most.[45,46] Decreases in Vickers hardness of the cortical bone in the present study were limited to 0.75 mm, which corresponds closely to the extent of the microfractures. Similarly, the greatest differences in bone density were obtained immediately adjacent to the MOP, where the density was ~10%-14% lower in the experimental than the control samples. Density differences between the experimental and control samples were <5% beyond 1.5 mm in both the cortical and trabecular samples. The fact that density differences extended farther than the microhardness differences shows that density more precisely measures the MOPs effects, probably because it is a 3D volumetric measurement taken at a resolution of 30 μm. Evaluating piezocision in rats, Dibart et al[28] reported demineralization extending ~2.5 mm, which may be due to greater amounts of trauma induced in rats, which would produce greater RAP effects.[34] As previously indicated, microfractures produced by the placement of MOPs decrease fluid shear stress within the canaliculi, leading to localized osteocyte death.[37-42] Apoptotic osteocytes are chemotactic for osteoclasts.[42,47] On that basis, there appears to be a threshold, around 5%, below which significant increases in tooth movement will not occur, limiting the clinically significant extent of the RAP produced by the placement of MOPs to ~1.5 mm.

Importantly, the MOPs also induce a biologically significant RAP effect farther away from the trauma sites. There were significant decreases in cortical and trabecular bone density in the experimental bone 3-4 mm from the MOP sites, and dramatic TRAP activity after 2 weeks ≥2.5 mm from the edges of the MOPs. The extent of this effect was particularly unexpected in cortical bone, which is metabolically less active than trabecular bone.[48,49] As previously discussed, osteocytes have multiple projections that allow them to communicate through the lacunocanalicular network that lies within the mineralized bone. Each dendritic process extends ~125 μm (0.125 mm) from the osteocyte, and each osteocyte in human bone has from 18 to 106 processes.[47] This results in the average osteocyte having a mean total cumulative length of ~4 mm.[47] Osteocytes also possess the ability to resorb bone within their individual lacunae.[49] However, unlike osteoclasts, they do not remove the osteoid matrix. Therefore, it is possible that the distant RAP observed in the present study was due to apoptotic osteocytes, located immediately adjacent to the MOP sites, sending out a signal through the canalicular network to initiate demineralization by distant osteocytes. This could be a mechanism for the mobilization of calcium, which is needed to repair the injured bone.

The clinical applicability of the present results relates to the MOPs' potential to accelerate tooth movements. The present findings indicate that a few MOPs placed >1-2 mm from the tooth should not be expected to have of much of an effect on rates of tooth movement. A recent experimental study showed that multiple MOPs placed 3-7 mm from the teeth being moved did not increase tooth movements after 7 weeks and had no effect on osteoblasts, osteoclasts, or mineralization of bone near the teeth being moved.[20] A recent randomized split-mouth study of 37 patients showed that canine retraction was no faster on the side that had 3 MOPs than on the control side.[19] For MOPs to accelerate tooth movements, many would have to be placed close together and close to the entire root surface.

The major limitation of the present study relates to its applicability to humans. Of the various species commonly used in research, including dogs, sheep, goat, pigs, and rabbits, the bone structure of dogs is most similar to humans.[23] The composition of dog bone has been shown to more closely approximate humans than sheep, pig, cow, or chicken bone.[21] However, rates of trabecular and cortical bone healing are faster in dogs than humans.[23] Regarding microstructure, Wang et al showed that dogs have more plexiform bone than humans, indicative of bone that grows at faster rates.[22] Another limitation of the study is its sample size. The small but consistent differences observed in cortical and trabecular bone density would probably have been statistically significant had the experiment been performed with more animals.

CONCLUSIONS

Within the limits of this study, when MOPs are performed in mandibular furcal bone of beagle dogs, and evaluations are performed after 2 and 4 weeks:

1. The demineralization effects of MOPs on bone are transient, and are not evident after 4 weeks.
2. Although bone density is decreased up to 4.2 mm, the principal effects do not extend more than 1.5 mm from the MOP.
3. MOP placement in cortical and trabecular bone produces extensive areas of acellular bone adjacent to the placement site.

4. Healing of the injured area and bone growth are evident 2 weeks after the trauma.
5. Normal trabecular healing occurs following MOP placement.

ACKNOWLEDGMENTS

This study was funded by the Robert E. Gaylord Endowed Chair in Orthodontics.

REFERENCES

1. Buschang P, Campbell P, Russo S. Accelerating tooth movement with corticotomies: is it possible and desirable? Semin Orthod 2012;18:286-94.
2. Skidmore KJ, Brook KJ, Thomson WM, Harding WJ. Factors influencing treatment time in orthodontic patients. Am J Orthod Dentofacial Orthop 2006;129:230-8.
3. Beckwith FR, Ackerman RJ Jr, Cobb CM, Tira DE. An evaluation of factors affecting duration of orthodontic treatment. Am J Orthod Dentofacial Orthop 1999;115:439-47.
4. Årtun J, Brobakken BO. Prevalence of carious white spots after orthodontic treatment with multibonded appliances. Eur J Orthod 1986;8:229-34.
5. Segal GR, Schiffman PH, Tuncay OC. Meta analysis of the treatment-related factors of external apical root resorption. Orthod Craniofac Res 2004;7:71-8.
6. Ristic M, Svabic MV, Sasic M, Zelic O. Clinical and microbiological effects of fixed orthodontic appliances on periodontal tissues in adolescents. Orthod Craniofac Res 2007;10:187-95.
7. Roberts WE, Huja S, Roberts JA. Bone modeling: biomechanics, molecular mechanisms, and clinical perspectives. Semin Orthod 2004;10:123-61.
8. Iwasaki LR, Haack JE, Nickel JC, Morton J. Human tooth movement in response to continuous stress of low magnitude. Am J Orthod Dentofacial Orthop 2000;117:175-83.
9. Nightingale C, Jones SP. A clinical investigation of force delivery systems for orthodontic space closure. J Orthod 2003;30:229-36.
10. Frost HM. The regional acceleratory phenomenon: a review. Henry Ford Hosp Med J 1983;31:3-9.
11. Sebaoun JD, Kantarci A, Turner JW, Carvalho RS, van Dyke TE, Ferguson DJ. Modeling of trabecular bone and lamina dura following selective alveolar decortication in rats. J Periodontol 2008;79:1679-88.
12. Wilcko MT, Wilcko WM, Pulver JJ, Bissada NF, Bouquot JE. Accelerated osteogenic orthodontics technique: a 1-stage surgically facilitated rapid orthodontic technique with alveolar augmentation. J Oral Maxillofac Surg 2009;67:2149-59.
13. Mostafa YA, Mohamed Salah Fayed M, Mehanni S, ElBokle NN, Heider AM. Comparison of corticotomy-facilitated vs standard tooth-movement techniques in dogs with miniscrews as anchor units. Am J Orthod Dentofacial Orthop 2009;136:570-7.
14. Alikhani M, Raptis M, Zoldan B, Sangsuwon C, Lee YB, Alyami B, et al. Effect of micro-osteoperforations on the rate of tooth movement. Am J Orthod Dentofacial Orthop 2013;144:639-48.
15. Baloul SS, Gerstenfeld LC, Morgan EF, Carvalho RS, van Dyke TE, Kantarci A. Mechanism of action and morphologic changes in the alveolar bone in response to selective alveolar decortication-facilitated tooth movement. Am J Orthod Dentofacial Orthop 2011;139:S83-101.
16. Safavi SM, Heidarpour M, Izadi SS, Heidarpour M. Effects of flapless bur decortications on movement velocity of dogs' teeth. Dent Res J (Isfahan) 2012;9:783-9.
17. Swapp A, Campbell PM, Spears R, Buschang PH. Flapless cortical bone damage has no effect on medullary bone mesial to teeth being moved. Am J Orthod Dentofacial Orthop 2015;147:547-58.
18. Teixeira CC, Khoo E, Tran J, Chartres I, Liu Y, Thant LM, et al. Cytokine expression and accelerated tooth movement. J Dent Res 2010;89:1135-41.
19. Alkebsi A, Al-Maaitah E, Al-Shorman H, Abu Alhaija E. Three-dimensional assessment of the effect of micro-osteoperformations on the rate of tooth movement during canine retraction in adults with Class II malocclusion: a randomized controlled clinical trial. Am J Orthod Dentofacial Orhtop 2018;153:771-85.
20. Cramer CL, Campbell PM, Opperman LA, Tadlock LP, Buschang PH. The effects of micro-osteoperformations on tooth movements and bone in the beagle maxilla. Am J Orthod Dentofacial Orthop 2018;155:681-92.
21. Aerssens J, Boonen S, Lowet G, Dequeker J. Interspecies differences in bone composition, density, and quality: potential implications for in vivo bone research. Endocrinology 1998;139:663-70.
22. Wang X, Mabrey JD, Agrawal CM. An interspecies comparison of bone fracture properties. Biomed Mater Eng 1998;8:1-9.
23. Pearce AI, Richards RG, Milz S, Schneider E, Pearce SG. Animal models for implant biomaterial research in bone: a review. Eur Cells Mater 2007;13:1-10.
24. Landrigan MD, Li J, Turnbull TL, Burr DB, Niebur GL, Roeder RK. Contrast-enhanced micro–computed tomography of fatigue microdamage accumulation in human cortical bone. Bone 2011;48:443-50.
25. Dall'Ara E, Ohman C, Baleani M, Viceconti M. The effect of tissue condition and applied load on Vickers hardness of human trabecular bone. J Biomech 2007;40:3267-70.
26. Boivin G, Bala Y, Doublier A, Farlay D, Ste-Marie LG, Meunier PJ, et al. The role of mineralization and organic matrix in the microhardness of bone tissue from controls and osteoporotic patients. Bone 2008;43:532-8.
27. Goldstein H. Multilevel models in educations and social research. London: Oxford University Press; 1987.
28. Dibart S, Yee C, Surmenian J, Sebaoun JD, Baloul S, Goguet-Surmenian E, et al. Tissue response during Piezocision-assisted tooth movement: a histological study in rats. Eur J Orthod 2014;36:457-64.
29. Iino S, Sakoda S, Ito G, Nishimori T, Ikeda T, Miyawaki S. Acceleration of orthodontic tooth movement by alveolar corticotomy in the dog. Am J Orthod Dentofacial Orthop 2007;131:448.e1-8.
30. Sanjideh PA, Rossouw PE, Campbell PM, Opperman LA, Buschang PH. Tooth movements in foxhounds after one or two alveolar corticotomies. Eur J Orthod 2010;32:106-13.
31. Kim SJ, Park YG, Kang SG. Effects of Corticision on paradental remodeling in orthodontic tooth movement. Angle Orthod 2009;79:284-91.
32. Berglundh T, Abrahamsson I, Lang NP, Lindhe J. De novo alveolar bone formation adjacent to endosseous implants. Clin Oral Implants Res 2003;14:251-62.
33. Shefelbine SJ, Augat P, Claes L, Simon U. Trabecular bone fracture healing simulation with finite element analysis and fuzzy logic. J Biomech 2005;38:2440-50.
34. McBride MD, Campbell PM, Opperman LA, Dechow PC, Buschang PH. How does the amount of surgical insult affect

bone around moving teeth? Am J Orthod Dentofacial Orthop 2014;145:S92-9.
35. Spencer AC, Campbell PM, Dechow P, Ellis ML, Buschang PH. How does the rate of dentoalveolar distraction affect the bone regenerate produced? Am J Orthod Dentofacial Orthop 2011;140:e211-21.
36. Moore C, Campbell PM, Dechow PC, Ellis ML, Buschang PH. Effects of latency on the quality and quantity of bone produced by dentoalveolar distraction osteogenesis. Am J Orthod Dentofacial Orthop 2011;140:470-8.
37. Clarke B. Normal bone anatomy and physiology. Clin J Am Soc Nephrol 2008;3:S131-9.
38. Verbruggen SW, Vaughan TJ, McNamara LM. Fluid flow in the osteocyte mechanical environment: a fluid-structure interaction approach. Biomech Model Mechanobiol 2014;13:85-97.
39. Park J-S, Yu W, Kyung H-M, Kwon O-W. Finite element analysis of cortical bone strain induced by self-drilling placement of orthodontic microimplant. Korean J Orthod 2009;39:203-12.
40. Yu W, Park HS, Kyung HM, Kwon OW. Dynamic simulation of the self-tapping insertion process of orthodontic microimplants into cortical bone with a 3-dimensional finite element method. Am J Orthod Dentofacial Orthop 2012;142:834-41.
41. Li H, Liang CZ, Shen CC, Chen QX. Decreases in fluid shear stress due to microcracks: a possible primary pathogenesis of Kummell's disease. Med Hypotheses 2011;77:897-9.
42. Jahani M, Genever PG, Patton RJ, Ahwal F, Fagan MJ. The effect of osteocyte apoptosis on signalling in the osteocyte and bone lining cell network: a computer simulation. J Biomech 2012;45:2876-83.
43. Zainal Ariffin SH, Yamamoto Z, Zainol Abidin lZ, Megat Abdul Wahab R, Zainal Ariffin Z. Cellular and molecular changes in orthodontic tooth movement. ScientificWorldJournal 2011;11:1788-803.
44. Graber LWV, Robert L Jr, Vig KWL. Orthodontics: current principles and techniques. Philadelphia, Pa: Mosby; 2012.
45. Lee NK, Baek SH. Effects of the diameter and shape of orthodontic mini-implants on microdamage to the cortical bone. Am J Orthod Dentofacial Orthop 2010;138:8.e1-8: discussion 8-9.
46. Yadav S, Upadhyay M, Liu S, Roberts E, Neace WP, Nanda R. Microdamage of the cortical bone during mini-implant insertion with self-drilling and self-tapping techniques: a randomized controlled trial. Am J Orthod Dentofacial Orthop 2012;141:538-46.
47. Buenzli PR, Sims NA. Quantifying the osteocyte network in the human skeleton. Bone 2015;75:144-50.
48. Kini U, Nandeesh BN. Physiology of bone formation, remodeling, and metabolism. In: Fogelman I, Gnanasegaran G, Wall H, editors. Radionuclide and hybrid bone imaging. Berlin and Heidelberg: Springe; 2012. p. 29-57.
49. Bilezikian JP. Principles of bone biology. Academic Press; 2002.